Study on the Shear Failure of Reinforced Concrete Beams Using Extended Finite Element Method (XFEM)

Hanadi Abdulridha Lateef [1,*], Rafil Mahmood Laftah [2], Nabeel Abdulrazzaq Jasim [3]

[1] Department of Structure and Construction, Basrah Technical Institute, Southern Technical University, Basrah, Iraq
[2] Department of Mechanical Engineering, College of Engineering, University of Basrah, Basrah, Iraq
[3] Department of Civil Engineering, College of Engineering, University of Basrah, Basrah, Iraq
E-mail addresses: hanadi.ridha@stu.edu.iq , rafil.laftah@uobasrah.edu.iq , nabeel_ali58@yahoo.com

Abstract

This research concerns with the fracture behavior of reinforced concrete beams without shear reinforcement numerically. The software ABAQUS is adapted to simulate the crack propagation using the eXtended Finite Element Method (XFEM), taking into account materials nonlinearities using concrete damage plasticity CDP criteria. XFEM is used to solve the discontinuity problems in the simulation. The maximum principal stress failure criterion is selected for damage initiation, and an energy-based damage evolution law based on a model-independent fracture criterion is selected for damage propagation. The traditional nonlinear finite element analysis is used to specify the crack initiation position, which is required to specify the crack location in the analysis of beams using XFEM. Three-dimensional reinforced concrete beam models are investigated subjected to three and four-point loading tests. Simply supported beams under the effect of applied static load are investigated. An elastic perfectly plastic model is used for modeling the longitudinal steel bars. The main variables considered in the study are beam depth and the shear span with beam length. The numerical results are compared with the available experimental results to demonstrate the applicability of the model. The XFEM provides the capability to predict the concrete member fracture behavior.

Keywords: Concrete Damage Plasticity, Fracture Energy, Shear Span, XFEM.

1. Introduction

Since the end of the nineteenth century and the beginning of the twentieth century, concepts of fracture mechanics were beginning to appear depending on experimental and theoretical studies [1]. Fracture mechanics is the study of the mechanical behavior of cracked materials subjected to an applied load. The formation of cracks may be a complex fracture process, which strongly depends on the microstructure of a particular crystalline or amorphous solid, applied loading, and environment. The failure in concrete can occur by the growth of cracks gradually during loading. As the load is increasing, cracks increase in number and grow until one of the cracks will propagate through the member [2]. The shear failure is very dangerous because it happens suddenly with little or no previous warning. The shear design must ensure that the shear strength for every member in the structure exceeds the flexural strength. The shear failure mechanism varies depending upon the cross-sectional dimensions, the member properties, the geometry, and the loading types [3]. The numerical simulation of crack propagation and the analysis of crack growth in reinforced concrete members is still an unsolved problem and an important part of current research. The development of reliable analytical models can reduce the number of required test specimens for the solution of a given problem, recognizing that tests are time-consuming and costly and often do not simulate exactly the loading and support conditions of the actual structure. Full-scale simulations of structural systems which cannot be produced and tested in a laboratory cannot be produced and tested in a laboratory environment can result in a better understanding of the failure and cracking behavior of these systems. Many computer software packages are available for these simulations. The commercially available ABAQUS software has dedicated concrete material models that are quite effective in realistic simulations [4]. Recent advancements in computational simulations have paved the possibility for carrying out the design and analysis of concrete structures in a more realistic manner.

Many researchers have used numerical methods to study the fracture behavior of members. In 1999, Belytschko and Moës suggested a new computational method named the "extended finite element method (X-FEM)" [5]. Belytschko with Black in 1999 and Moës et al., 1999, produced a substantial perfection to the basis of traditional FEM to simulate the crack without modification of the initial finite element mesh. After that, the modifications of the method continued to be used in various problems such as localized deformation, discontinuous field, fracture, and so on. It has become widely used in civil engineering and other fields because it offers a good simulation. Then, Moës et al. 1999 produced the Heaviside function and crack tip function as the enrichment shape function of elements including the crack surface and tip respectively. Later, Daux et al. in 2000, utilized more than one enrichment shape function in crack tip

elements, and crack branching was successfully simulated. Later, a new crack nucleation criterion was introduced into X-FEM by Belytschko et al. 2003. The crack propagation path and velocity can be well predicted using this criterion as cited in Ref. [6]. Giner et al. in 2009 [7] used XFEM with the finite element software ABAQUS to simulate the fracture mechanism for the two-dimensional model. User Element subroutine (UEL) was used for combining XFEM with classical FEM because XFEM was not included in the ABAQUS program at that time. In 2011, Johannsson [8] dealt with the modeling of cracks in a three-dimensional reinforced concrete beam subjected to three-point bending in the ABAQUS program. XFEM was used to model the cracking in cooperation with the Concrete Damaged Plasticity material model. Yang in 2016 [9], used the XFEM and FEM with concrete damage plasticity material models to predict the failure for a two-dimensional concrete beam with recycled aggregate. Al-Zuhairi and Taj in 2018 [10], investigated two-dimensional, simply supported, plain concrete beams under flexural stresses using meso-scale mode by XFEM with ABAQUS program for the numerical model. In 2020 [11], chen et al. was proposed the XFEM-based multiscale modeling approach to investigate the monotonic and hysteretic performance of RC columns and Ahmed et al. in 2021 [12], conducted the numerical modelling of foamed concrete beam under flexural using traction-separation relationship. The traction separation relationship was used as a constitutive model to incorporate independent material properties and used in the modelling framework.

More studies are required to understand the effect of many significant parameters on concrete beam behavior and carrying capacity such as change shear span and beam dimensions. The major objective of this research is to investigate the fracture mechanics of reinforced concrete beams numerically. First, the ultimate strength and load-deflection relationships, as well as crack patterns, are validated with the corresponding experimental results from the previous study carried out by Kornbak [13]. After the verification of the XFEM model, it is used for conducting a parametric study to determine the effect of some parameters on the behavior of reinforced concrete beams.

2. XFEM for crack simulation

In practice, discontinuities may be found in imperfections, cracks, shear bands and in many structural problems. Discontinuity can be classified into types: strong and weak discontinuity, which represent respectively the cracks and the interfaces between two different materials in structural concepts [14]. With the conventional finite element method, it is difficult to be analyzed the discontinuity that occurs in a concrete model. XFEM allows simulation of initiation and propagation of a discrete crack along an arbitrary solution path without the requirement of remeshing [15].

The major concept of this method is adding enrichment functions to the standard finite element analysis solution. It is based on the multiplication of the enrichment function by the nodal shape function. The technique of enrichment could be applied to a specific region of the general domain by enriching only within that region. Equations (1) and (2) below shown the final finite element approximation using enrichment functions [1].

$$u(x) = u^{FE} + u^{enr} \tag{1}$$

$$u(x) = \sum_{j=1}^{n} N_j(x)\, u_j + \sum_{k=1}^{m} N_k(x)\, \psi(x)\, a_k \tag{2}$$

where u_j is the vector of regular degrees of nodal freedom in the finite element method. a_k is the added set of degrees of freedom to the standard finite element model and ψ is the discontinuous enrichment function defined for the set of nodes that the discontinuity has in its influence (support) domain.

2.1. Level set method (LSM)

LSM is a numerical technique for describing a crack and tracking the motion of the crack. Combining XFEM with level sets improves the XFEM in modelling a growing crack or moving phase boundaries. The level set function consists of many types of functions, the most common function is the signed distance function. The level set approach was introduced by Osher [16]. In other words, the signed distance function can take one of the following values, Fig. 1 [17].

$$\varphi(x) = \begin{cases} > 0 \ \ if \ x \in \Omega_A \\ = 0 \ \ if \ x \in \Gamma_d \\ < 0 \ \ if \ x \in \Omega_B \end{cases} \tag{3}$$
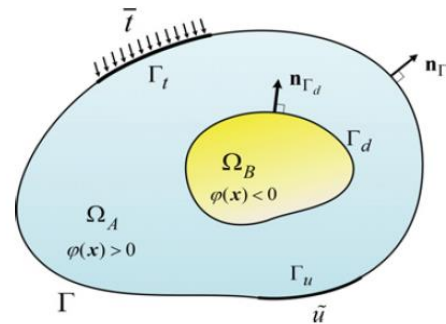

Fig. 1 Domain with weak discontinuity defined by a bi-material with close interface [15].

2.2. Enrichment functions

To solve discontinuities problems, the XFEM relies on the Partition of Unity (PU) technique. Equation (4) illustrates how the enrichment functions are added to the convenient solution in the PU method. There are a number of different enrichment options available. Heaviside enrichment function (HSF), $H(x)$ is commonly used for strong discontinuities such as crack. It was first introduced by Moe's [5].

Strong discontinuities can be created when the displacement of one side of the crack interface is different from the other, this led to a discontinuity in the solution. HSF can take two approaches as follows [15]:

$$H(x) = \begin{cases} 0 \ \ if \ \varphi(x) < 0 \\ 1 \ \ if \ \varphi(x) > 0 \end{cases} \tag{4}$$

or,

$$H(x) = \begin{cases} -1 \ \ if \ \varphi(x) < 0 \\ +1 \ \ if \ \varphi(x) > 0 \end{cases} \tag{5}$$

Where, $\varphi(x)$ is the signed distance function illustrated in the previous section.

Table 1. The characteristics of concrete and steel.

Concrete Characteristics			Steel Characteristics			
Compressive Strength $f_c{}'$ (MPa)	Poisson's ratio (v)	Density (kg/m^3)	Yielding Stress f_y (MPa)	Modulus of elasticity E_s (GPa)	Poisson's ratio (v)	Cross-sectional area (mm^2)
43	0.2	2350	533	190	0.3	88.356

For the purpose of validation of the extended finite element model, experimental test available in literature is utilized.

3. Experimental analysis of beam

The beam tested by Kornbak [13] is used to demonstrate the applicability of the FE model. The concrete beam was simply supported singly reinforced and without transverse reinforcement. The longitudinal reinforcement was two number 7.5 mm diameter ribbed bars. The cross section of beam was 100×100 mm as shown in Fig. 2. The figure depicts the geometry, loading, and boundary conditions of the beam. The properties of the concrete and steel are summarized in Table 1. The failure crack was located at 20 mm from the support as obtained from the experimental test. The load was applied at the midspan on the top surface of the beam by a plate of area 50 mm × 100 mm.
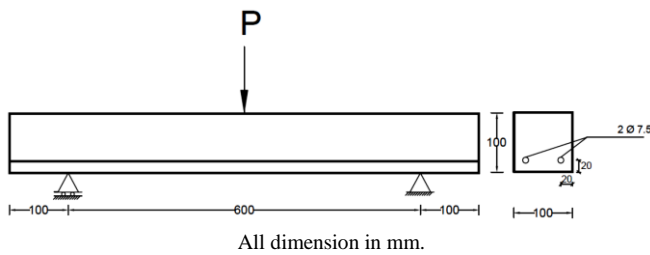

All dimension in mm.

Fig. 2 The details and a cross-section of the reinforced concrete beam.

4. Finite element modelling

Finite element simulations of reinforced concrete beams are performed using commercial software ABAQUS/Standard 2017. Materials nonlinearity is taken into account.

4.1. Materials properties

Non-linearity in concrete due to its complex composition has been given thought in this constitutive modeling to faithfully capture the response of concrete [18]. In this paper, the concrete damage plasticity CDP model is used to describe the concrete beam behavior. The nonlinear stress-strain relationship of concrete in compression is presented in Fig. 3.
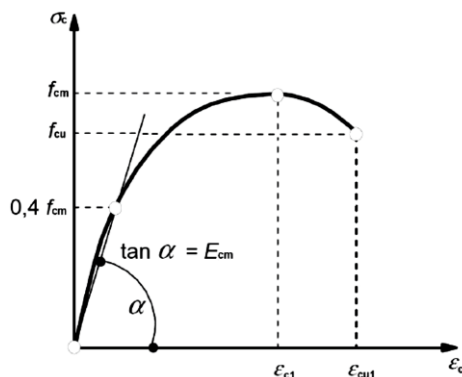

Fig. 3 The nonlinear stress-strain relationship of concrete in compression, Eurocode 2 (2004).

The elastic properties of the concrete are determined by the modulus of elasticity and the Poisson's ratio (v). The modulus of elasticity of concrete (E_{cm}) is calculated based on the prescribed relation in Eurocode 2 (2004) [19],

$$E_{cm} = 22000 \left(\frac{f_{cm}}{10}\right)^{0.3} \quad \text{(in MPa)} \tag{6}$$

$$f_{cm} = f_{ck} + 8 \quad \text{(in MPa)} \tag{7}$$

where, f_{cm} is the cylinder concrete compressive strength (mean value) and f_{ck} is the characteristic cylinder concrete compressive strength at 28 days.

Using Eurocode 2 (2004) [19], the hardening region was found in the uniaxial compression of concrete as,

$$\sigma_c = f_{cm} \left[\frac{k\eta - \eta^2}{1 + (k - 2)\eta}\right] \tag{8}$$

Where,

$$\eta = \frac{\varepsilon_c}{\varepsilon_{c1}} \tag{9}$$

and

$$k = \frac{1.05 \, E_{cm} \, |\varepsilon_{c1}|}{f_{cm}} \tag{10}$$

σ_c is the concrete compressive strength for $0 < |\varepsilon_c| < \varepsilon_{cu1}$, ε_c is the concrete compressive strain, ε_{c1} is the compressive strain of concrete at peak stress f_{cm} and ε_{cu1} is the ultimate compressive strain in the concrete. The Eurocode 2 (2004) [19] specified that the ultimate strain for characteristic compressive strength of concrete between 12-50 MPa, can be taken as 0.0035. For ε_{c1}, Majewski proposed approximating formula to calculate ε_{c1} depending on the experimental result as cited in Ref. [20], from the following expression:

$$\varepsilon_{c1} = 0.0014 \, (2 - e^{-0.024 f_{cm}} - e^{-0.14 f_{cm}}) \tag{11}$$

The tensile stress is calculated according to Eurocode 2 (2004) [19] as:

$$\sigma_t = f_t \left(\frac{\varepsilon_t}{\varepsilon}\right)^{0.4} \tag{12}$$

where ε_t is the tensile strain in the concrete at the peak stress f_t, ε is the tensile strain in the concrete and f_t is the concrete tensile strength, which is expressed by the following relationship as in Eurocode 2 (2004) [19]:

$$f_t = 0.30 \, (f_{ck})^{2/3} \tag{13}$$

The stiffness degradations coefficients for the concrete damaged plasticity material model for compression (d_c) and tension (d_t) are another important parameter in the damage plasticity model available in ABAQUS. They describe the evolution of the concrete stresses when the concrete material reaches peak stress. Numerous methods are available to achieve the damage parameter. Nguyen and Kim (2009) [21] presented the following relations for defining prescribed parameters, $d_c = 1 − \sigma_c/f_{cm}$ and $d_t = 1 − \sigma_t/f_t$ for compression and tension, respectively. The parameters of CDP model that are used in the current study are listed in Table 2.

Table 2. Parameters of CDP model under compound stress.

Parameter name	Value
Dilatation angle	38°
Eccentricity	0.1
f_{bo} /f_{co}	1.16
K	0.667
Viscosity parameter	0.0001

In the finite element model, an elastic perfectly plastic model was used for the steel longitudinal bars with an equal behavior in tension and compression. ABAQUS software requires input data of Young modulus (E_s) and Poisson's ratio (v) to represent the elastic behavior, yield stress (f_y), and the inelastic strains for defining the plasticity behavior as shown in Fig. 4.
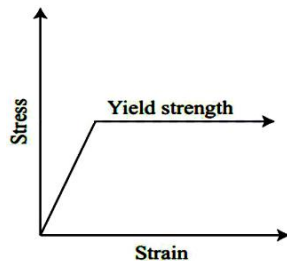
Fig. 4 Behavior of steel.

4.2. Types of used elements

The concrete beam is modeled with solid elements (C3D8R) from the ABAQUS library. They are eight-node elements with three translation degrees of freedom at each node, and of reduced integration with hourglass control. To simulate reinforcement bars, the truss element (T3D2) is adopted. It is 2-noded elements having 3 degrees of freedom in each node (translations in X, Y and Z directions). In this work, frictional contact between the steel and concrete in ABAQUS was achieved by using embedded technology [22].

4.3. Boundary and loading conditions

The load is displacement controlled; the displacement is applied downwards as pressure. The boundary conditions in roller support are U1 = U2 = 0, and in hinge support U1 = U2 = U3 = 0, where U: 1, 2, 3 are the translations in the X, Y and Z directions.

4.4. Crack initiation criteria and crack length

Crack initiation criteria must be specified in the XFEM. In this study, the maximum principal stress damage is used with a value of the ultimate tensile strength f_t as maximum principal stress at cracking. The f_t is determined by Equation (13) based on Eurocode 2 [19]. The fracture energy G_f may be estimated from the compressive strength of concrete and maximum aggregate size according to CEB-FIP MC 90 [23], as:

$$G_f = G_{f_0} \left(\frac{f_{cm}}{f_{cmo}}\right)^{0.7} \tag{14}$$

Where, G_f is fracture energy (N/mm), G_{f0} is the base value of fracture energy which depends on maximum aggregate size d_{max} as given in Table 3, f_{cm} is the mean value of concrete cylinder compressive strength (MPa) and f_{cmo} equals 10 MPa. Fracture energy (G_f) is calculated depending on the maximum aggregate size d_{max} of 10 mm as used in the experimental test [13]. The resulting fracture energy from Equation (14) equals 0.072 N/mm.

Table 3. The base value of G_{f0}

d_{max} (mm)	8	16	32
G_{fo} (N/mm)	0.025	0.030	0.058

To determine the suitable predefined crack length which gives results with acceptable accuracy compared with the experimental study, three beams with different initial crack lengths are studied, which are 5 mm, 10 mm and 15 mm. Table 4 summarized the results of different crack lengths. The ultimate load of the beam with crack length of 5 mm is very close to the ultimate load in the experimental test. Therefore, the crack length of 5 mm is used throughout this study.

Table 4. Variation of ultimate load with different crack lengths.

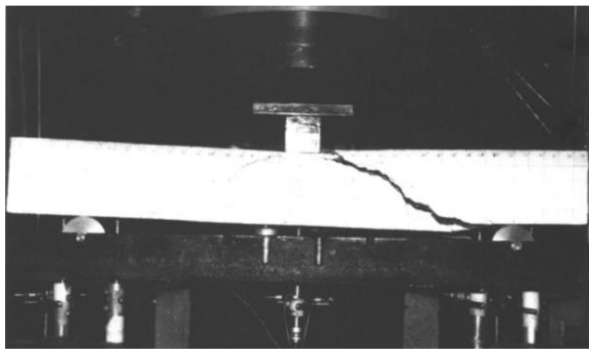| Crack Length (mm)	Ultimate Load (kN) XFEM	Load Ratio	Ultimate Load (kN) Exp.
5	27.5	1	
10	26.4	0.96	28.6
15	25.7	0.94	

4.5. Mesh size

Six models with different mesh sizes are examined to select a suitable mesh size which gives results with acceptable accuracy compared with the experimental study. The main parameters considered for this purpose are the ultimate load and the failure mode. The results of the study are presented in Table 5. It has been found that model (5) gives acceptable results for the ultimate load. The failure mode and crack propagation which are obtained experimentally along with those given by XFEM for model (5) are shown in Fig. 5. The load-deflection relationships, the experimental and numerical, are depicted in Fig. 6. Therefore, model (5) is used throughout this study.
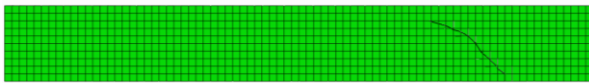
**Table 5.** Results of models with different element sizes and the ultimate load of the experimental beam.

Model No.	No. of Elements	No. of Nodes	Ultimate Load (kN) XFEM	Ultimate Load (kN) Exp.
(1)	234	432	24.1	
(2)	512	825	25.8	
(3)	1025	1512	26.8	28.6
(4)	2597	3456	27.1	
(5)	8000	9922	27.5	
(6)	64000	71001	27.9	

(a)

(b)

Fig. 5 The crack propagation under loading, **(a)** shear failure in the experimental test, and **(b)** crack path numerically by XFEM.
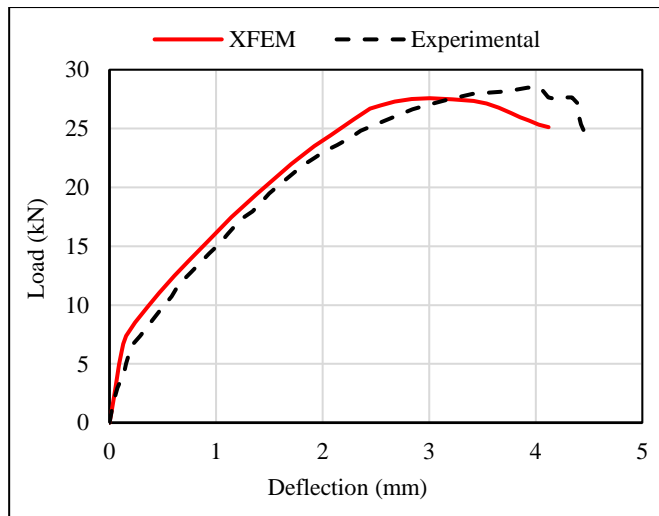
Fig. 6 Variation of mid-span deflection with load for model (5).

5. Results and Discussions

The main variables considered in the study were beam depth and the shear span with a beam length.

5.1. Influence of change in beam depth

To investigate the influence of the change of the beam depth under the three-point bending test, six beams are studied with similar properties and geometry, but with different depths. The beams are longitudinally reinforced with two bars with a diameter of 7.5 mm as the beam in the experimental test. The material properties of the concrete and steel are

summarized in Table 1. The depths of investigated beams are 100 mm, 150 mm, 200 mm, 250 mm, 300 mm, and 350 mm.

The numerical results are compared with the results of Bažant and Kim equation (obtained by approximate nonlinear fracture mechanics method) [24], which is given as:

$$P_u = 2 V_u \, B \, W \tag{15}$$

$$V_u = \frac{8 \, \rho^{1/3}}{\sqrt{1 + W/(25 \, d_{max})}} \left[\sqrt{f_{cm}} + 3000 \sqrt{\rho / \left(\frac{S}{2W} \right)^5} \right] \tag{16}$$

In which f_{cm} and V_u are in psi.
P_u = the shear strength.
$\rho = A_s /(B \, W)$, reinforcement ratio.
S = effective length of the beam.
W = the height of the beam.
B = the width of the beam.
d_{max} = maximum aggregate size.

The numerical results are also compared with the provisions of the ACI code (318-19) [25]. The ACI equation for nominal concrete shear strength provided by concrete for $A_v < A_{v \, min.}$ is:

$$V_c = \left[0.66 \, \lambda \, \lambda_s \, (\rho_w)^{1/3} \sqrt{f_{cm}} \right] b_w \quad \text{(in N)} \tag{17}$$

Where,
λ = modification factor (equal 1 for normal concrete).
λ_s = factor used to modify shear strength based on the effects of member depth and given by:

$$\lambda_s = \sqrt{\frac{2}{1 + 0.004 \, d}} \le 1 \tag{18}$$

ρ_w = steel ratio = $A_s / b_w . d$
b_w = the beam width, mm.
d = the beam depth, mm.
f_{cm} = cylinder concrete compressive strength (in MPa).

The results of the six beams are summarized in Table 6, including the cracks distances and the load value associated with the first crack and the failure crack. The first crack distance for all the beams is approximately 290 mm from the support, but the load value associated with the first crack is different for each beam. The ratios of the first crack load to the ultimate load are in the range of 0.25 to 0.46.

Table 6. The results of traditional nonlinear FEM, XFEM and ACI code for beams with different depths.

Beam Height (mm)	FEM					XFEM		Bažant & Kim Eq. (10)	ACI Eq. (12)	Failure Type
	* First Crack Distance (mm)	First Crack Load (kN)	* Failure Crack Distance (mm)	Ultimate Load (kN)	** Load Ratio	* Failure Crack Distance (mm)	Ultimate Load (kN)	Ultimate Load (kN)	Ultimate Load (kN)	
100	290	7.1	20	28.9	0.25	20	27.5	18.6	15.4	Shear
150	290	15	20	45.8	0.33	20	43.9	28.1	21.4	Shear
200	290	27.1	30	67.6	0.40	30	65.2	40.6	26.4	Shear
250	290	37.7	30	87.6	0.43	30	85.2	56.8	31.2	Shear
300	290	47.7	60	110.5	0.43	60	108.3	77.1	34.4	Shear
350	290	55	290	119.7	0.46	290	111.3	101.8	36.8	Bending

* The crack distance measured from the support.

$$** \text{ Load Ratio} = \frac{\text{First Crack Load}}{\text{Ultimate Load}}$$

The failure mechanism of the reinforced concrete beams is modelled quite well using XFEM and the failure load predicted is close to the failure load obtained by FEM analysis. Fig. 7 reveals that the load capacity increases with the increase in beam depth. This finding is obtained from the results of XFEM, Equation (15) and ACI-Equation (17). However, the maximum concrete shear stress decreases with the increase in beam depth for ACI-Equation (17) as shown in Fig. 8, but no clear relation is obtained from the results of XFEM and Equation (15).
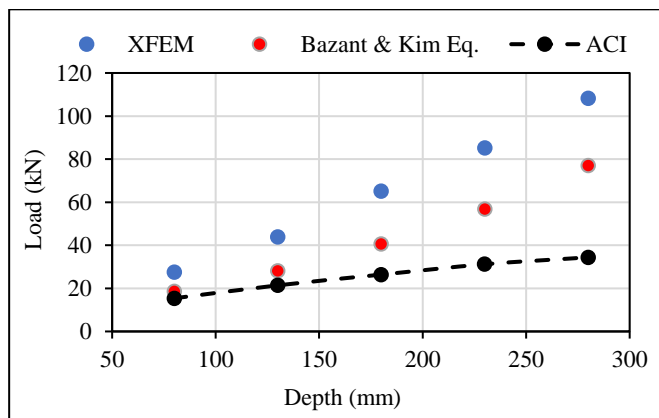
Fig. 7 Load versus beam depth relations for XFEM, Bažant and Kim Eq. and ACI code.
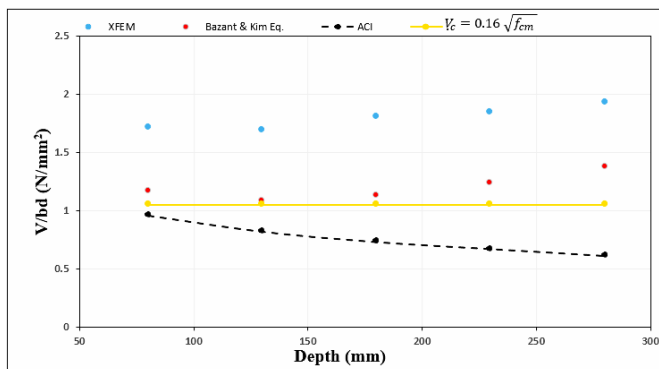
Fig. 8 Concrete strength versus beam depth relations for XFEM, Bažant and Kim Eq. and ACI code.

Depending on the change in the beam depth, different modes of failure are observed as shown in Fig. 9. Several micro-cracks appeared at the early stages of the loading process. These cracks extended and widened as the load is increased. Then cracks are developed at the middle region of the beam in the tension zone under applied load. After the flexural cracks, diagonal cracks appeared, causing the failure of the beam. It is observed that all investigated beams failed by shear except the last beam with a depth of 350 mm. This may be due to this beam acts as a deep beam. Deep beams are members that are loaded on one face and supported on the opposite face such that struts as compression members and ties develop between the load and supports, thus, it prevents shear failure. By the comparison of the crack propagation using XFEM with the crack pattern of the non-linear finite element method, it can be seen that the crack pattern is in good agreement for all the beams.

Figure 10 shows the relations between the loads and deflections. The first crack load and the ultimate load can also be observed for the beams with different depths. All beams seem to have a similar response, especially in the elastic region. The results of nonlinear FEM and XFEM are in reasonable agreement.

5.2. Influence of change in shear span

Analysis is also conducted to investigate the influence of the change in the beam length and the influence of the shear span on diagonal crack propagation and the load-carrying capacity of the beams. Two different shear spans are examined, which are $L/3$ and $L/4$, L is beam length. The investigated concrete beams are simply supported under two symmetrical concentrated loads and reinforced with longitudinal reinforcement without shear reinforcement. The beams are longitudinally reinforced with four bars with a diameter of 20 mm. The details and the cross-section of the tested reinforced concrete beams are shown in Fig. 11. The distance S is equal to 100 mm for beams with $L = 1000$ mm to 3000 mm and 250 mm for beams with $L = 4000$ mm to 6000 mm, $a = L/3$ and $L/4$. The material properties of the concrete and steel are summarized in Table 7. The initial crack is of 5 mm length. Due to the symmetry, the three-dimensional analysis is performed on one-half of the beam length and appropriate boundary conditions are applied on the cuts as shown in Fig. 12. The symmetry of the beams is in the Z-direction therefore U3 = UR1 = UR2 = 0, where U3 is the translation in the Z-direction, UR:1, 2 are the rotation about X and Y axes respectively.
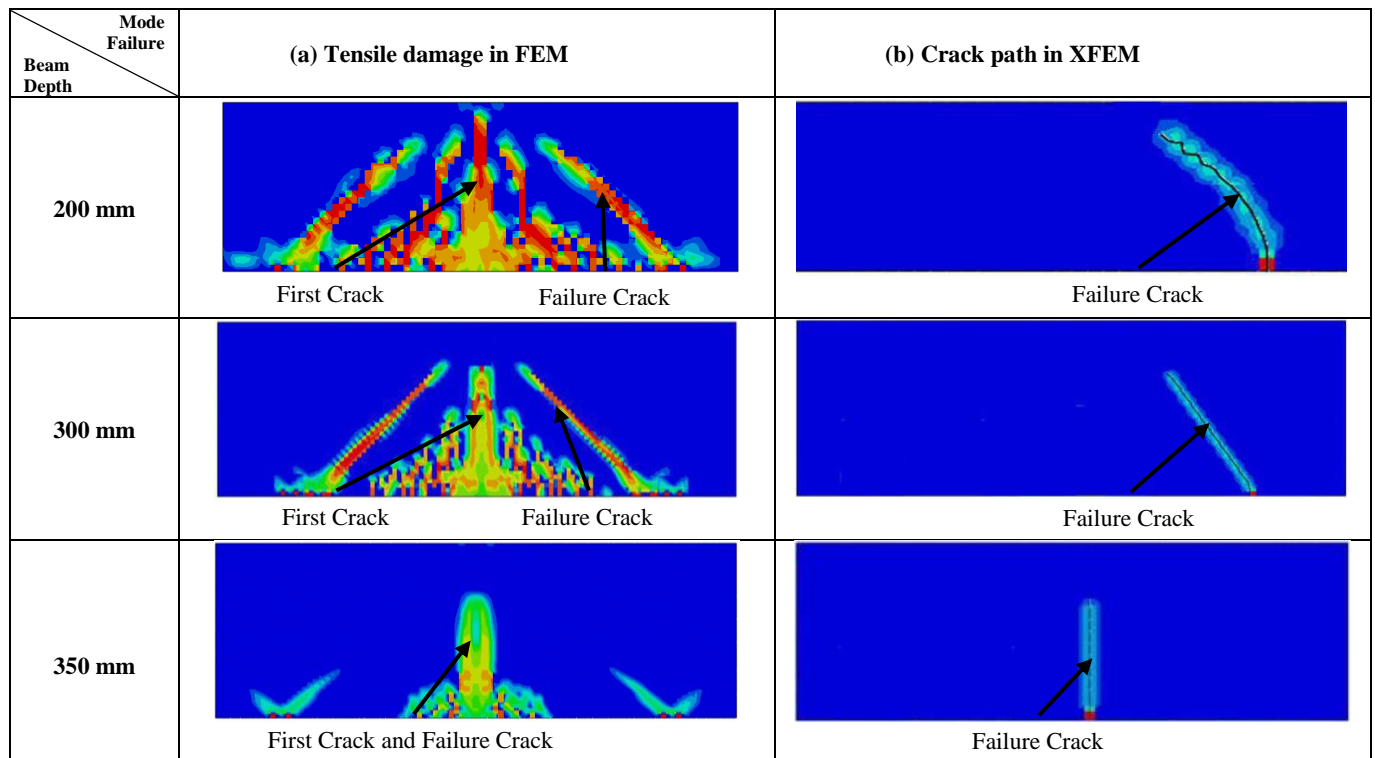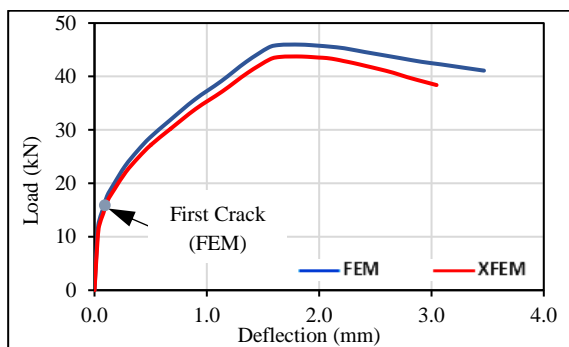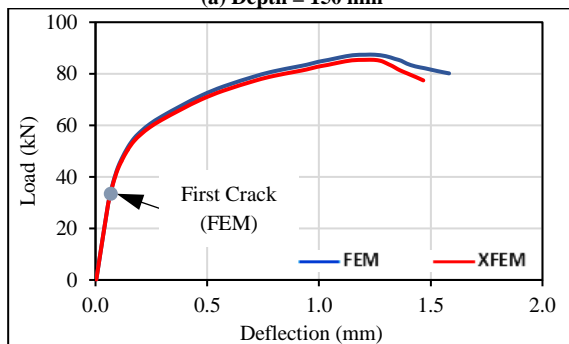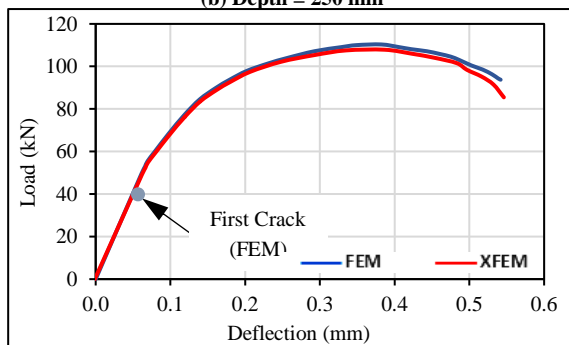
Mode Failure / Beam Depth	(a) Tensile damage in FEM	(b) Crack path in XFEM
200 mm	First Crack Failure Crack	Failure Crack
300 mm	First Crack Failure Crack	Failure Crack
350 mm	First Crack and Failure Crack	Failure Crack

Fig. 9 Crack pattern for beams with different depths using **(a)** FEM and **(b)** XFEM.

(a) Depth = 150 mm

(b) Depth = 250 mm

(c) Depth = 300 mm

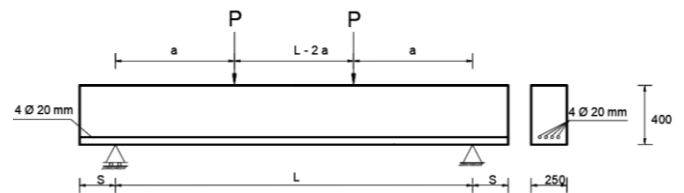**Fig. 10** Load-deflection relations for beams with different depths.

Fig. 11 Setup of the beam and cross-section details.
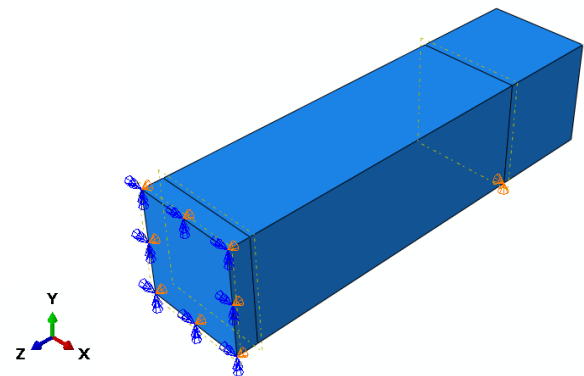
Fig. 12 ABAQUS model for half beam.

The results of the reinforced concrete beams with a shear span of $L/3$ and $L/4$ are summarized in Tables 8 and 9, respectively, including the cracks distances, and the load values associated with the first cracks and the failure cracks. The load ratios which are defined as first crack load/ultimate load for FEM and XFEM are in the range (0.4 - 0.49) and (0.38 - 0.47), respectively in beams with a shear span of $L/3$. While the first cracks of all beams appeared when the load reached (0.44 - 0.64) of the ultimate load in FEM and (0.41 - 0.63) in XFEM in beams with a shear span of $L/4$.

Table 7. The characteristics of concrete and steel.

Concrete Characteristics				Steel Characteristics			
Compressive Strength f_c' (MPa)	Poisson's ratio (v)	Density (kg/m³)	Fracture energy (N/mm)	Yielding Stress f_y (MPa)	Modulus of elasticity E_s (GPa)	Poisson's ratio (v)	Cross-sectional area (mm²) A_s
43	0.2	2400	0.072	570	200	0.3	1256.64

Table 8. FEM and XFEM results of RC beams with different lengths under four-point loads and shear span = $L/3$.

Beam Length (mm)	FEM					XFEM				Failure Type
	* First Crack Distance (mm)	First Crack Load (kN)	* Failure Crack Distance (mm)	Ultimate Load (kN)	** Load Ratio	* First Crack Distance (mm)	First Crack Load (kN)	Ultimate Load (kN)	** Load Ratio	
1000	30	110.2	30	227.2	0.49	30	105.1	224.8	0.47	Shear
2000	750	103	30	220.5	0.46	750	99.8	210	0.47	Shear
3000	950	78.6	30	187	0.42	950	72.4	185.7	0.39	Shear
4000	1550	57.7	30	143.6	0.40	1550	53.2	140.1	0.38	Shear
5000	1550	41.6	1350	102.6	0.41	1550	39.2	99.3	0.39	Bending
6000	1900	34.6	1725	76	0.45	1900	31.9	73.4	0.43	Bending

Table 9. FEM and XFEM results of RC beams with different lengths under four-point loads and shear span = $L/4$.

Beam Length (mm)	FEM					XFEM				Failure Type
	* First Crack Distance (mm)	First Crack Load (kN)	* Failure Crack Distance (mm)	Ultimate Load (kN)	** Load Ratio	* First Crack Distance (mm)	First Crack Load (kN)	Ultimate Load (kN)	** Load Ratio	
1000	20	165	30	259	0.64	20	162.7	256.8	0.63	Shear
2000	500	120.8	30	235	0.52	500	116.9	230	0.51	Shear
3000	750	110	30	212	0.52	750	107	210.8	0.51	Shear
4000	975	77.5	30	167	0.46	975	72.9	165	0.44	Shear
5000	1150	56.8	700	130	0.43	1150	52.7	126	0.42	Shear
6000	1825	42.7	1675	96.5	0.44	1825	39.6	95	0.42	Bending

* The crack distance measured from the support.

** Load Ratio = $\dfrac{\text{First Crack Load}}{\text{Ultimate Load}}$

The failure mode of the reinforced concrete beams with a shear span of $L/3$ and $L/4$ for both the FEA and XFEM are depicted in Figs. 13 and 14, respectively. There was a good agreement between the results of the FEA and the XFEM for the concrete crack patterns.

The variation of the deflection with the load of the reinforced concrete beams with a shear span of $L/3$ and $L/4$ for both the FEA and XFEM are depicted in Figs. 15 and 16, respectively. In general, the load-deflection relations obtained from the FEM results show an excellent agreement with those of the XFEM.

According to the results above for beams with different lengths and different loading conditions, the shear strength of simply supported beams is significantly influenced by the shear span. The loading condition is the primary parameter that significantly influenced the shear failure mechanism in concrete beams reinforced longitudinally and without transverse reinforcement. In general, with increasing the shear span, the failure loads and consequently the shear strength of the examined beams decreased as shown in Fig. 17. It can be seen that a linear relation exists between the ultimate load and beam length for different shear spans. The correlation coefficient R^2 for the obtained linear equations are (0.9867) and (0.9773) for shear spans $L/4$ and $L/3$ respectively. Considering the results of XFEM, the obtained equations are:

For shear span $L/3$:
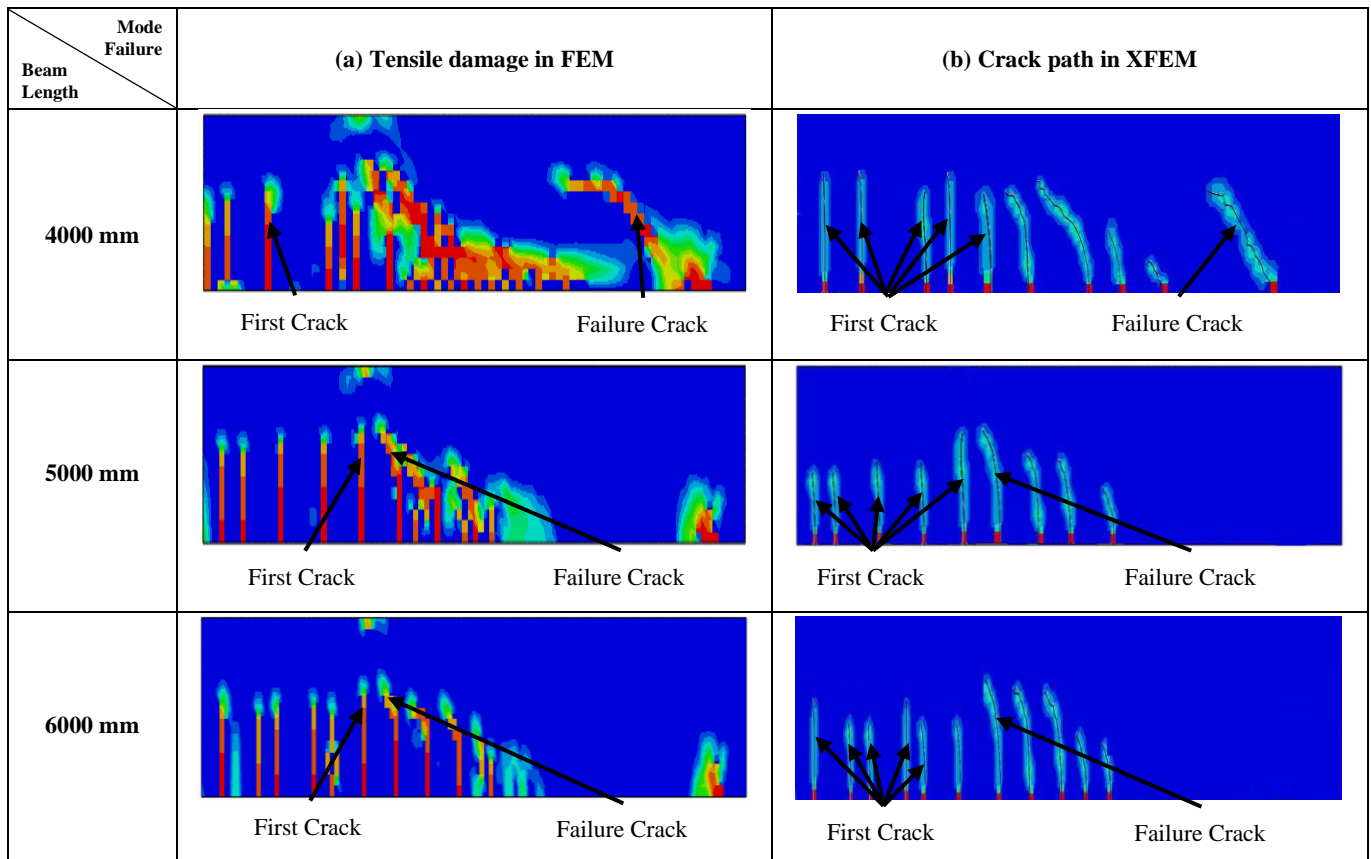
$P = -0.0324\,L + 269.02$　which may be simplified to
$P = -L/31 + 269$
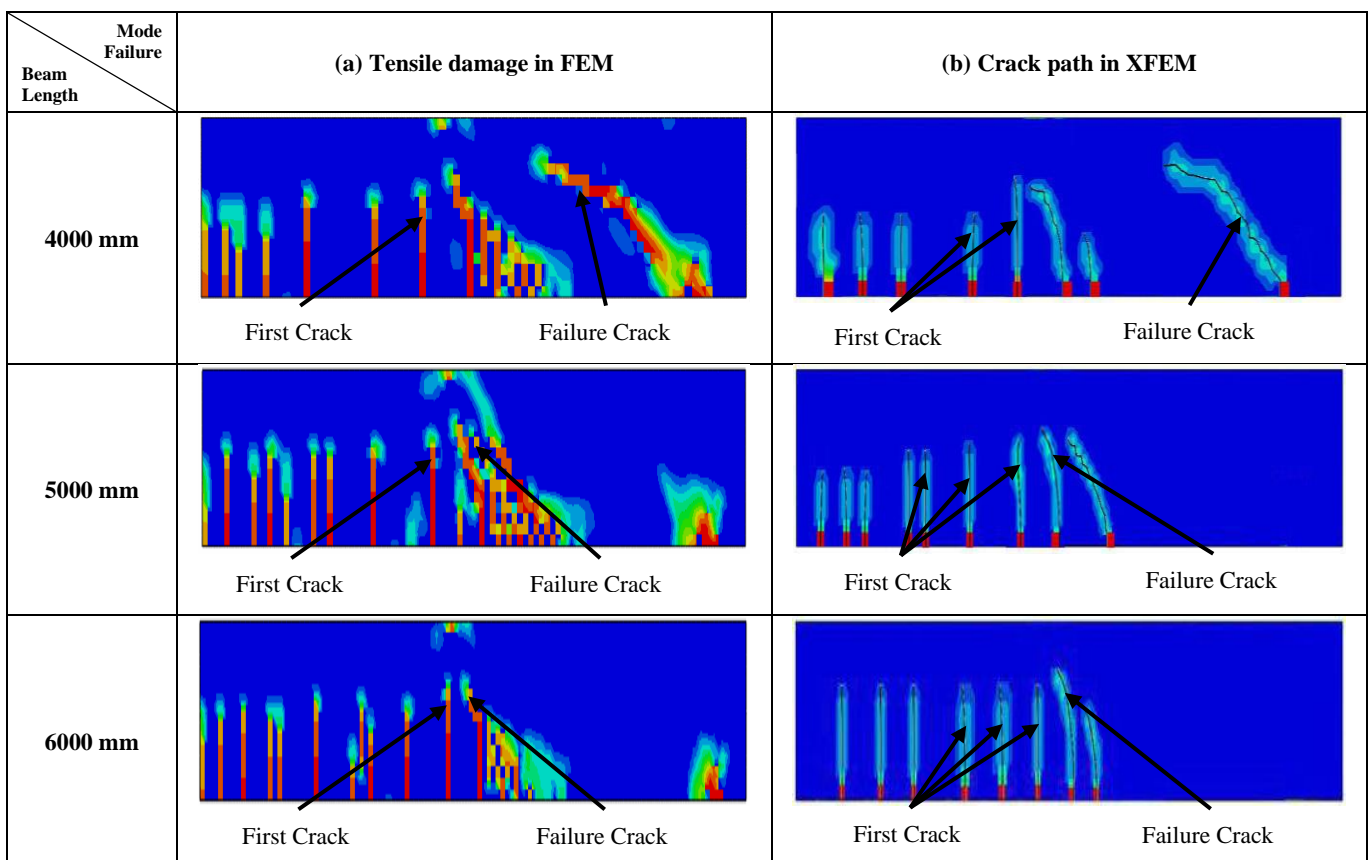
For shear span $L/4$:

$P = -0.0333\,L + 297.28$　which may be simplified to
$P = -L/30 + 297$

where P is the ultimate load in kN (shear) and L is the effective span of the beam in mm.

The two straight lines in Fig. 11 are approximately parallel therefore, the increase in shear strength is about 10 % (= 297/269 - 1) when the shear span reduces by 25 %.

Mode Failure / Beam Length	(a) Tensile damage in FEM	(b) Crack path in XFEM
4000 mm	First Crack — Failure Crack	First Crack — Failure Crack
5000 mm	First Crack — Failure Crack	First Crack — Failure Crack
6000 mm	First Crack — Failure Crack	First Crack — Failure Crack

Fig. 13 Crack pattern for the beams shear span = $L/3$ using **(a)** FEM and **(b)** XFEM.

Mode Failure / Beam Length	(a) Tensile damage in FEM	(b) Crack path in XFEM
4000 mm	First Crack — Failure Crack	First Crack — Failure Crack
5000 mm	First Crack — Failure Crack	First Crack — Failure Crack
6000 mm	First Crack — Failure Crack	First Crack — Failure Crack

Fig. 14 Crack pattern for the beams shear span = $L/4$ using **(a)** FEM and **(b)** XFEM.

6. Conclusions

Three-dimensional reinforced concrete beam models are investigated using XFEM, taking into account materials nonlinearities using concrete damage plasticity CDP. From the results obtained, the following conclusions may be drawn:

1. A fracture mechanics approach based on the XFEM can capture crack propagation leading to shear failure.
2. Because of the predefined crack in XFEM, the ultimate loads of the beams are less than the load values of nonlinear FEM by 1 % to 5 %.
3. The numerical analysis shows that the first crack distance for all the beams with different depths is approximately 290 mm from the support, but the load value associated with the first crack is different for each beam. The ratios of the first crack load to the ultimate load are in the range of 0.25 to 0.46.
4. The loading condition is the significant parameter that affects the shear failure mechanism in reinforced concrete beams. The failure loads and consequently the shear strength of the examined beams decreased with increasing the shear span. The increase in shear strength is about 10 % when the shear span is reduced by 25 %.
5. The load ratios which are defined as first crack load/ ultimate load for FEM and XFEM are in the range (0.4 - 0.49) and (0.38 - 0.47), respectively for reinforced concrete beams with shear span $L/3$. While the load ratios for reinforced concrete beams with shear span $L/4$, are in the range (0.44 - 0.64) and (0.41 - 0.63) for FEM and XFEM respectively.

References

[1] S. Mohammadi, Extended Finite Element Method for Fracture Analysis of Structures, Published by Blackwell, UK, First Edition, ISBN: 978-0-470-69779-5, 2008.

[2] Y. B. Zaitsev, and F. H. Wittmann, "Simulation of crack propagation and failure of concrete", Matériaux et Construction, Vol. 14, pp. 357-365, 1981. https://doi.org/10.1007/BF02478729

[3] M. M. Al-Nasra, and N. M. Asha, "Shear Reinforcements in the Reinforced Concrete Beams", American Journal of Engineering Research (AJER), Vol. 2, Issue 10, pp. 191-199, 2013. https://www.ajer.org/papers/v2(10)/V0210191199.pdf

[4] Y. Dere, and M. A. Koroglu, "Nonlinear FE Modeling of Reinforced Concrete", International Journal of Structural and Civil Engineering Research, Vol. 6, No. 1, pp.71-74, 2017. https://doi.org/10.18178/ijscer.6.1.71-74

[5] N. Moës, J. Dolbow, T. Belytschko, "A finite element method for crack growth without remeshing", International Journal for Numerical Methods in Engineering, Wiley, Vol. 46, Issue 1, pp.131-150, 1999. https://doi.org/10.1002/(SICI)1097-0207(19990910)46:1<131::AID-NME726>3.0.CO;2-J

[6] Z. Zhuang, Z. Liu, B. Cheng, and J. Liao, Extended Finite Element Method, Published by Elsevier Inc, First Edition, 2014. https://doi.org/10.1016/C2012-0-01326-9

[7] E. Giner, N. Sukumar, and F. J. Fuenmayor, "An Abaqus Implementation of the Extended Finite Element Method", Engineering Fracture Mechanics, Vol. 76, Issue 3, pp. 347-368, 2009. https://doi.org/10.1016/j.engfracmech.2008.10.015

[8] B. Johannsson, "Numerical Analysis of a Reinforced Concrete Beam in Abaqus 6.10", M. Sc. Thesis, Aalborg University, 2011. https://pdfslide.net/documents/numerical-analysis-of-a-reinforced-concrete-beam-in-abaqus-610.html

[9] W. Yang, "Modeling Recycled Aggregate Concrete Crack by Extended Finite Element Method and Concrete Damage Plasticity", M. Sc. Thesis, The University of Tennessee at Chattanooga, Chattanooga, Tennessee, 2016. https://scholar.utc.edu/cgi/viewcontent.cgi?article=1606&context=theses

[10] A. H. Al-Zuhairi, and A. I. Taj, "Finite Element Analysis of Concrete Beam under Flexural Stresses Using Meso-Scale Model", Civil Engineering Journal, Vol. 4, No. 6, pp.1288-1302, 2018. https://www.civilejournal.org/index.php/cej/article/view/821

[11] H. Chen, B. Xu, J. Wang, X. Nie, and Y-L. Mo, "XFEM-Based Multiscale Simulation on Monotonic and Hysteretic Behavior of Reinforced-Concrete Columns", Applied Science, Vol. 10, No. 21, pp. 1-20, 2020. https://doi.org/10.3390/app10217899

[12] H. Ahmad, S. Sugiman, Z. M. Jaini, and A. Z. Omar, "Numerical Modelling of Foamed Concrete Beam under Flexural Using Traction-Separation Relationship", Latin American Journal of Solids and Structures, Vol. 18, No. 5, pp.1-13, 2021. https://doi.org/10.1590/1679-78256330

[13] D. Lange-Kornbak, and B. L. Karihaloo, "Fracture Mechanical Prediction of Transitional Failure and Strength of Singly- reinforced Beams", European Structural Integrity Society, Vol. 24, pp. 31-66, 1999. https://doi.org/10.1016/S1566-1369(99)80061-2

[14] A. R. Khoei, Extended Finite Element Method: Theory and Applications, John Wiley & Sons, Ltd., First Edition, 2015. https://doi.org/10.1002/9781118869673

[15] S. Mohammadi, XFEM Fracture Analysis of Composites, A John Wiley & Sons, Ltd., First Edition, 2012. https://doi.org/10.1002/9781118443378

[16] S. Osher, and J. A. Sethian, "Fronts Propagating with Curvature-Dependent Speed: Algorithms Based on Hamilton–Jacobi Formulations", Journal of Computational Physics, Vol. 79, Issue 1, pp. 12-49, 1988. https://doi.org/10.1016/0021-9991(88)90002-2

[17] F. E. A. Abaqus, "ABAQUS analysis user's manual", Dassault Systems, Broekaart, USA, 2012. http://130.149.89.49:2080/v6.12/pdf_books/ANALYSIS_2.pdf

[18] J. George, S. K. Rama, M. S. Kumar, and A. Vasan, "Behavior of Plain Concrete Beam Subjected to Three Point Bending using Concrete Damaged Plasticity (CDP) Model", Materials Today: Proceedings, Vol. 4, Issue 9, pp. 9742-9746, 2017. https://doi.org/10.1016/j.matpr.2017.06.259

[19] Eurocode 2, "Design of concrete structures - part 1-1: general rules and rules for buildings", British Standards Institution, London, 2004. https://www.phd.eng.br/wp-content/uploads/2015/12/en.1992.1.1.2004.pdf

[20] P. Kmiecik, and M. Kaminski, "Modelling of Reinforced Concrete Structures and Composite Structures with Concrete Strength Degradation Taken into Consideration", Archives of Civil and Mechanical Engineering, Vol. 11, Issue 3, pp. 623-636, 2011. https://doi.org/10.1016/S1644-9665(12)60105-8

[21] H.T. Nguyen, and S.E. Kim, "Finite Element Modeling of Push-out Tests for Large Stud Shear Connectors", Journal of Constructional Steel Research, Vol. 65, Issues 10-11, pp. 1909-1920, 2009. https://doi.org/10.1016/j.jcsr.2009.06.010

[22] B.I. Karlsson, and E.P. Sorensen, "ABAQUS Analysis User's Guide Volume IV: Elements", Pawtucket, Rhode Island, Hibbitt Publication, 2006.

[23] The FIB Model Code for Concrete structures, CEB-FIP Model Code 90, London, First Edition, 1993.

[24] Z. P. Bažant, and J. K. Kim, "Size Effect in Shear Failure of Longitudinally Reinforced Beams", ACI Journal, Vol. 81, Issue 5, pp. 456-468, 1984. http://www.civil.northwestern.edu/people/bazant/PDFs/Papers/172.pdf

[25] ACI Committee 549, "Building Code Requirements for Structural Concrete", ACI 318R-19.